arXiv:1609.08875v1 [astro-ph.GA] 28 Sep 2016

Manuscript for *Revista Mexicana de Astronomía y Astrofísica* (2007)

SNR RADIO SPECTRAL INDEX DISTRIBUTION AND ITS CORRELATION WITH POLARIZATION: A CASE STUDY OF LUPUS LOOP

V. Borka Jovanović,[1] P. Jovanović,[2] and D. Borka[1]

Draft version: September 29, 2016

RESUMEN

ABSTRACT

We use radio-continuum all-sky surveys at 1420 and 408 MHz with the aim to investigate properties of the Galactic radio source Lupus Loop. The survey data at 1435 MHz, with the linear polarization of the southern sky, is also used. We calculate properties of this supernova remnant: the brightness temperature, surface brightness and radio spectral index. For determining borders and calculation of its properties, we use the method we have developed. The non-thermal nature of its radiation is confirmed. The distribution of spectral index over its area is also given. A significant correlation between the radio spectral index distribution and the corresponding polarized intensity distribution inside the loop borders is found, indicating that the polarization maps could provide us information about the distribution of interstellar medium, and thus could represent one additional way to search for new Galactic loops.

Key Words: ISM: supernova remnants — radiation mechanisms: non-thermal — radio continuum: ISM

1. INTRODUCTION

Radio surveys of the region in vicinity of the supernova of 1006 A.D. revealed a plateau or spur running out from the galactic plane near $l = 330°$ which contains two shell-like objects: Lupus Loop and SN1006 (Milne 1971). The general diffuse appearance of the Lupus Loop suggested that it is the remnant of a very old supernova (which is consistent with its low surface brightness) and these two remnants are not associated in any way (Milne & Dickel 1974). It was indicated earlier (Spoelstra 1973) that expanding sphere of the supernova remnants (SNRs) leads to compression of the interstellar magnetic field, which results in an observable radio source, and that the spatial orientation of the loops contains information on the direction of the magnetic field of the undisturbed medium outside the shell. Spoelstra (1973) treated the Lupus Loop as an object similar to the main Galactic loops, and found that it indicates magnetic field direction parallel to field found from Loop I. Radio continuum observations of this source are given in Milne (1971); Milne & Dickel (1974), radio line observations in Colomb & Dubner (1982),

[1]Vinča Institute of Nuclear Sciences, University of Belgrade, Serbia.
[2]Astronomical Observatory, Belgrade, Serbia.

X-ray observations and its spectrum can be found in Toor (1980); Leahy et al. (1991); Ozaki et al. (1994); Kaplan et al. (2006) and references therein, while far UV observations are presented in Shinn et al. (2006).

The analysis on the filamentary structure observed in polarization by WMAP (Wilkinson Microwave Anisotropy Probe) satellite is given in Vidal et al. (2015); Vidal (2016). It is described there that most of the polarized emission (at high latitudes) comes from individual filamentary features, and some of these structures are the well-known continuum radio loops. Using WMAP data at 23, 33 and 41 GHz, they studied the diffuse polarized emission over the entire sky, and they obtained the (average) polarization spectral indices which are consistent with synchrotron radiation.

A catalogue of Galactic SNRs, with some statistics of their parameters, is presented in Green (2014a), along with more detailed web-based version (Green 2014b). The current version of the catalogue contains 294 SNRs, and is based on research in the published literature up to the end of 2013. Lupus Loop, with catalogue name G330.0+15.0, is listed there, and some of its parameters are given. This low surface brightness loop has been observed in radio and X-ray wavelength range (Green 2014b).

Our aim is to study the properties of this remnant, and to calculate radio spectral index using the method we have previously developed. Our method of calculation is explained in detail in Borka Jovanović (2012) and references therein: we investigated Galactic Loops I-VI in papers Borka (2006); Borka Jovanović, Milogradov-Turin & Urošević (2006); Borka (2007), Borka, Milogradov-Turin & Urošević (2008); Borka Jovanović & Urošević (2010); Urošević & Borka Jovanović (2011), and we investigated smaller remnants in Borka Jovanović & Urošević (2008, 2009a,b, 2010, 2011), Borka, Borka Jovanović & Urošević (2012). This method is applicable to extragalactic radio sources as well (Borka Jovanović et al. 2012). In this paper we also want to investigate the nature of its radiation and to study how spectral index varies across the face of the remnant. Besides, we want to analyze and study the polarization of this SNR and to investigate its connection with the spectral index.

2. LUPUS LOOP AREA

2.1. *Temperature brightness contours*

We use the radio continuum surveys of the sky provided by Max Planck Institute for Radio Astronomy (MPIfR), Bon, Germany, available at the internet site: `http://www3.mpifr-bonn.mpg.de/survey.html`. Observational data, which we use for our calculations, are obtained from continuum radio emission at: 1420 MHz (Reich, Testori & Reich 2001) and 408 MHz (Haslam et al. 1982). At the frequency of 34.5 MHz (Dwarakanath & Udaya Shankar 1990) the loop could not be resolved. The angular resolutions of the surveys are: 35' at 1420 MHz and 0°.85 at 408 MHz, which give the corresponding observations at the rates, for both l and b, (1/4)° (1420 MHz) and (1/3)° (408

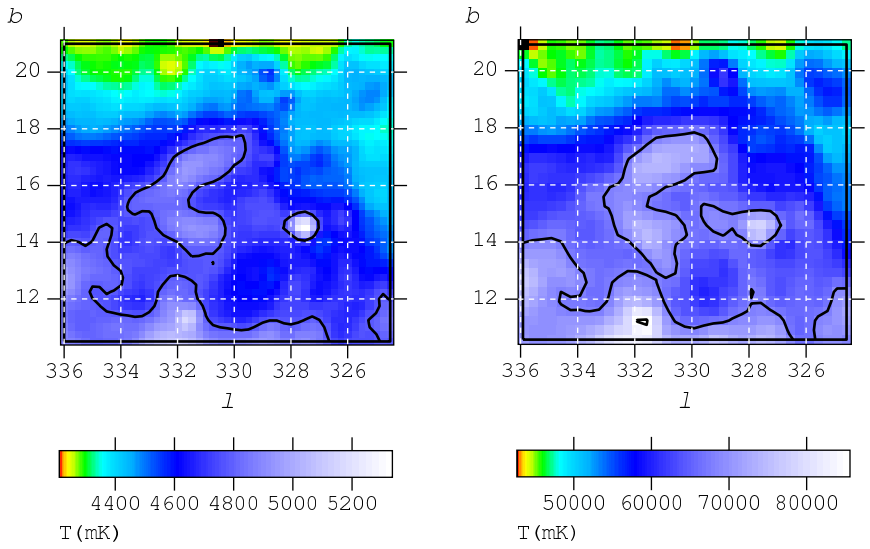

Fig. 1. Lupus Loop area with brightness temperature contour at 1420 MHz **(left)** and 408 MHz **(right)**. The contour is representing T_{min} as given in the Table 1. Below, the temperature scales are given (in mK).

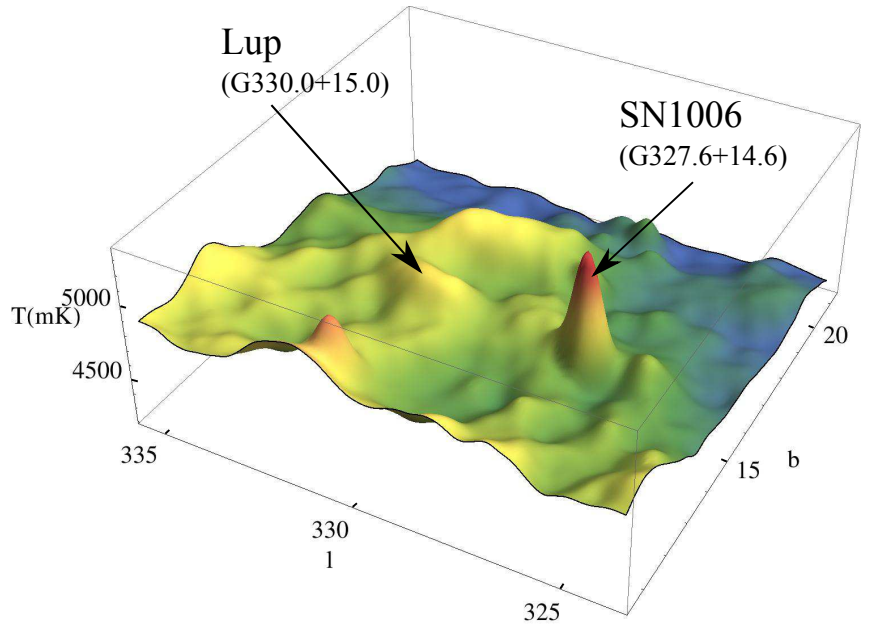

Fig. 2. The 3D map of the Lupus Loop and its surrounding at 1420 MHz. The brightness temperature is given in mK.

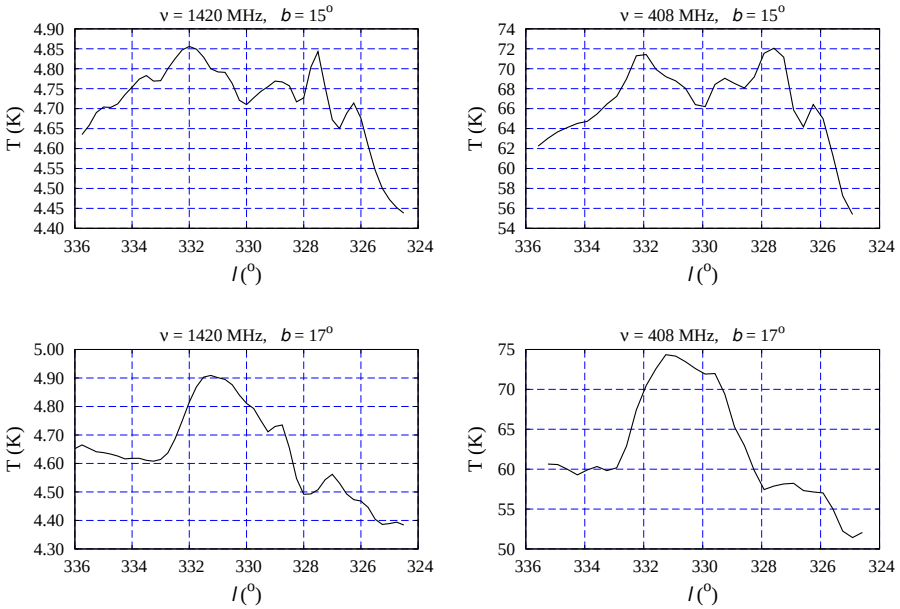

Fig. 3. **Left:** 1420 MHz temperature profiles for area containing Lupus Loop at galactic longitude $b = 15°$ (top) and 17° (bottom). **Right:** 408 MHz temperature profiles for $b = 15°$ (top) and 17° (bottom).

MHz). The effective sensitivities for average brightness temperature (T_b) are about 50 mK (1420 MHz) and 1.0 K (408 MHz).

As we showed earlier (Borka Jovanović (2012) and references therein), the method for defining a loop border and for determining the values of temperature and brightness, which we developed for main Galactic Loops I-VI, could be applicable to all SNRs. In that way we have determined the Lupus Loop area which is shown in Fig. 1. There is also influence of some other radio sources in the vicinity of the Lupus, regarding the determination of its radio properties, like brightness and radio spectral index. The 3D plot showing brightness temperatures of this loop and its surrounding, at the frequency of 1420 MHz, we show in Fig. 2. To make this figure more clear, we denoted the ridges of Lup and SN1006 with arrows. In Fig. 3 we want to demonstrate a few temperature profiles. Note that temperature peak around $l = 328°$ corresponds to another source (SN1006), and that we have to pay attention to the part of the profiles from $l = 334°$ to 329° to see how it changes over the Lupus SNR.

2.2. *Brightness temperatures and surface brightnesses*

Minimum and maximum brightness temperatures are given in Table 1. We use these values to determine the loop borders, and then, after subtracting the background emission over the Lupus area, we determine its brightness temperature T_b. Assuming the spectra to have a power-law form, i.e. the

TABLE 1

TEMPERATURE BORDERS, TEMPERATURES AND BRIGHTNESSES OF THE LUPUS LOOP AT 1420 AND 408 MHZ. THE BRIGHTNESSES ARE REDUCED TO 1000 MHZ WITH THE SPECTRAL INDEX WE CALCULATED: $\alpha = 0.98$.

frequency (MHz)	T_{min} (K)	T_{max} (K)	temperature (K)	brightness (10^{-23} W/(m^2 Hz sr))	brightness reduced to 1000 MHz (10^{-23} W/(m^2 Hz sr))
1420	4.78	5.4	0.10 ± 0.05	0.63 ± 0.31	8.82 ± 4.36
408	67.8	85	4.1 ± 1.0	2.12 ± 0.51	8.82 ± 2.13

flux density to be proportional to the frequency $S_\nu \propto \nu^{-\alpha}$ (or $T_b \propto \nu^{-\beta}$), using data of at least two frequencies, we can calculate radio spectral index α (or $\beta = \alpha + 2$) by fitting this equation to the data. Knowing two values of brightnesses (derived in this paper, at 1420 and 408 MHz), we obtained radio spectral index $\alpha = 0.98$. Using the relation:

$$\Sigma_\nu = 2kT_{b,\nu}(\nu/c)^2, \tag{1}$$

where k is the Boltzmann constant and c the speed of light, we calculate the surface brightness Σ_ν, and with

$$\Sigma_{1000}/\Sigma_\nu = (1000/\nu)^{-\alpha} \tag{2}$$

we finally obtain the values reduced at 1000 MHz. The results are listed in Table 1.

3. RADIO SPECTRAL INDEX

We calculated the mean value of the radio spectral index between 1420 and 408 MHz. With $\alpha = 0.98$, we confirmed non-thermal emission of radiation for this remnant. Our motivation is also to study how spectral index varies across its area. The distribution of radio spectral indices, over the Lupus Loop area, is shown in Fig. 4.

If we compare our value for α with earlier results, these new observations yielded a greater value. Milne (1971) calculated spectral index between the following frequencies: 5000, 2700, 1614, 1410, 635, 408 and 160 MHz, and obtained mean value $\alpha = 0.38$, while Milne & Dickel (1974) used data at 2700, 1660 and 1410 MHz which resulted in $\alpha = 0.5$, but we have to stress that they mentioned that conclusions about Lupus Loop were uncertain and that more data were required. Our result is larger than the typical value for Galactic SNRs, but in Green's catalogue regarding spectral index about 0.5 it is mentioned that it is not precisely determined, and there is also a question mark as a notice that it should be recalculated. Previous authors probably

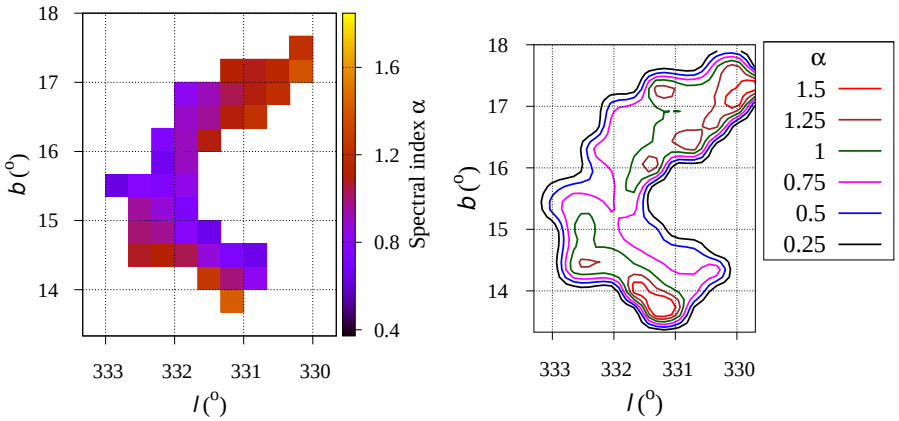

Fig. 4. Radio spectral index distribution across the Lupus Loop between 1420 and 408 MHz, in form of color map (***left***) and interpolated contours (***right***).

took into account wider area for Lupus Loop (i.e. loop together with one part of the background which is outside the border) and in that way they lowered the brightness temperature, as well as the mean spectral index. Also, there is a noticeable tendency for more recent observations to give higher values of α than the previous.

Averaged values for measured spectral indices of all-sky Galactic radiation vary with frequencies. For example, $\alpha = 0.55$ between 45 and 408 MHz (Guzman et al. 2011), $\alpha = 0.71$ between 408 and 3200 MHz (Platania et al. 2003) and $\alpha = 1.01$ between 2300 and 3300 MHz (Davies et al. 2006). Spectral distribution of the remnant gives information about the distribution of energy of the relativistic electrons that produce the emission observed at given radio-frequencies. Like in the previously mentioned case of Galaxy radiation, averaged value of α depends on the frequencies. In that way we can also explain greater absolute value for α in our paper than in older results.

The very end of the Lupus Loop is mixed with strong external sources and it is very hard to resolve loop from the background in this region. If we take whole area of the loop we will get $\alpha = 0.98$ and so high value of index is probably because of influence of these additional strong radio sources, and the ridges of the loop. The largest part of Lupus area has spectral indices between 0.4 and 0.8. If we take the area of the loop without the area enclosed by $\alpha = 1$ line (see green line in Fig. 4), i.e. between the contours 0.4 and 1, we get the average spectral index $\alpha = 0.77$, which is much closer to the typical value for SNRs ($\alpha = 0.5$). This area of the loop is relatively clean from external sources and it indicates that the mean spectral index is highly influenced by the loop's ridges also. The spectral index variations must reflect differences in the acceleration process from place to place within the SNR. This indicates that the increased emissivity could be the result of particle acceleration in the SNR shock (see Zhang et al. (1997)). Although the spectral index determinations based on several frequencies should be more accurate than these based on two

frequencies, we improved method for extracting the background, and this is very important in these cases when there are confusing sources.

As it can be seen from Fig. 4, the distribution of radio spectral index tells us that its variation over the loop area is rather large. So, we think that distribution of spectral index over the loop is more adequate in description of the loop than the mean spectral index.

From the Fig. 4 it can also be seen that the largest part of the loop's area has radio spectral index between 0.4 and 0.8. Then, the greater values are connected with its ridges, and as a whole it gives the mean value 0.98.

4. THE POLARIZATION SURVEYS AND MAPS

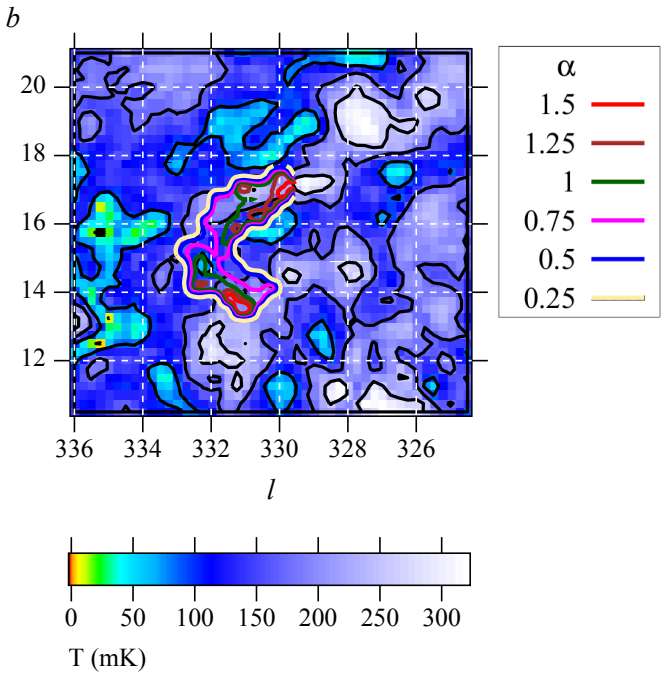

Fig. 5. Polarized intensity at 1435 MHz for the area surrounding Lupus Loop, shown in Galactic coordinates. Total intensity contours start at 10 mK T_b and run in steps of 80 mK T_b. The contour levels of α from Fig. 4 are superimposed.

If we want to measure the properties of the synchrotron radiation, it is very useful if we have the polarization data available, because the polarization of the mechanisms other than synchrotron is much smaller (see the comparison for the polarization of different mechanisms of radiation in Vidal et al. (2015)). Polarized electromagnetic radiation can be described using the Stokes parameters. We can use electric field (electromagnetic wave propagation) $\vec{E}$ and define Stokes parameters (I, Q, U, V) as time averages of the field (Vidal et al. 2015). Parameter I represents the total intensity of the field, parameters Q

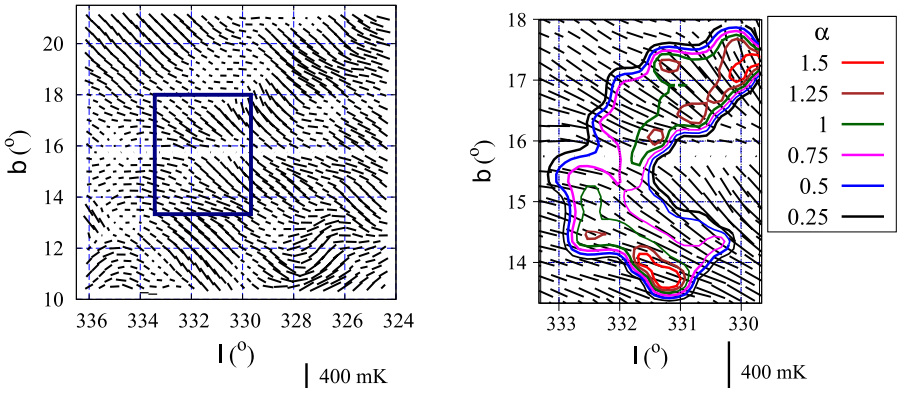

Fig. 6. **(*Left*:)** The distribution of the polarization $\vec{E}$ vectors at 1435 MHz over the same Lupus Loop area as in Fig. 1. The length of the vectors is proportional to the polarized intensities (see scale at the bottom). The inserted rectangular labels the (l,b) area which corresponds to Fig. 4. **(*Right*:)** A zoomed part of the figure, with the (l,b) intervals corresponding to Fig. 4. The contour levels of α from Fig. 4 are superimposed.

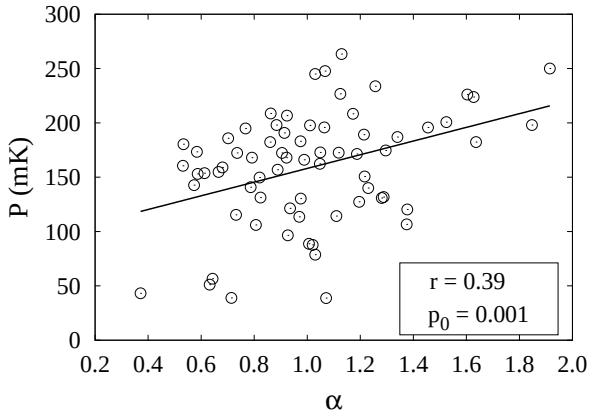

Fig. 7. Polarized intensity P at 1435 MHz versus spectral index α between 1420 and 408 MHz, calculated at the common positions (l, b) over the area of Lupus Loop, bounded by T_{min} and T_{max}. Open circles represent (α, P) pairs, and straight solid line their fit by linear function: $P(\alpha) = k\alpha + \bar{P}$. The values of correlation coefficient r and the significance level p_0 are denoted in the lower right corner of the figure.

and U represent the linear polarization, while V is the circular polarization. The polarized intensity is defined as:

$$P = \sqrt{Q^2 + U^2}, \tag{3}$$

with Q, U - the second and third Stokes parameters, which can be expressed by the polarization angle χ in the following form:

$$Q = P\cos 2\chi, \quad U = P\sin 2\chi. \tag{4}$$

The degree of polarization is given as:

$$p = S_p/(S_p + S_u) \tag{5}$$

where S_p is the flux density of the polarized component, and S_u of the unpolarized one.

The Villa Elisa survey data at 1435 MHz (Testori, Reich & Reich 2008), for linear polarization of the southern sky, are accessible via the MPIfR Survey Sampler. This linear polarization of Galactic synchrotron emission is given with the angular resolution of the survey of 35', that is, the observations are at the rates $(1/4)^\circ$ (for both l and b). The 1435 MHz polarized intensity for the area surrounding Lupus Loop, we show in Fig. 5. From the polarization survey in this figure we can see how the intensity is distributed, and we also have appended intensity contours. Besides, in order to make figure more clear, we presented the superimposing contour levels of α extracted from Fig. 4.

For comparison of the radio continuum survey with the observations of polarized emission, it is very useful if we present polarized intensities and the polarization angles (see Fig. 6): the polarized intensities are presented by the length of the vectors, and the polarization angles by their orientation.

5. DISCUSSION

Regarding the Figures 1 and 6 we can conclude that the polarization intensity is strongly correlated with brightness temperature, especially in the cases of 1420 MHz brightness temperature and the polarized intensity at 1435 MHz. Polarized emission is dominated by synchrotron radiation and because frequencies 1420 and 1435 MHz are very near each other, this correlation is expected. Polarization maps give us information about the interstellar distribution and it will also be one additional way to search for new Galactic loops.

Explanation of the large-scale polarization pattern is achieved using the model proposed by Heiles (1998). In this model, an expanded shell compresses the magnetic field in the local interstellar medium (ISM). Our results indicate that the magnetic field should be compressed by the supernova shock. The magnetic field of Lupus Loop is reflected magnetic field in the ambient interstellar medium (Heiles 1998; Platania et al. 2003; Davies et al. 2006; Guzman et al. 2011).

Dependence of polarized intensity P at 1435 MHz versus spectral index α between 1420 and 408 MHz over the area of Lupus Loop is presented in Fig. 7, suggesting a certain linear correlation between these two quantities. In order to estimate the significance of this linear dependence, we calculated the correlation coefficient r and the significance level p_0 at which the null hypothesis of zero correlation is disproved. The relatively high value obtained for r ($r = 0.39$) and small value for p_0 ($p_0 = 0.001$) both indicate that there is a significant linear correlation between polarized intensity P and spectral index α over the area of Lupus Loop as it can be also noticed from Fig. 6.

We also tested linear dependence between these two quantities by fitting their common values with the function $P(\alpha) = k\alpha + \bar{P}$ (solid straight line in Fig. 7). This fit resulted in the following values: $k = 63.0 \pm 18.4$ and $\bar{P} = 95.1 \pm 19.5$ (i.e. $\bar{P} \approx 100\bar{\alpha}$, where $\bar{\alpha}$ is the previously determined mean spectral index over the area of Lupus Loop).

We have confirmed previous theory (Spoelstra 1973) that the spatial orientation of the loops contains information on the direction of the magnetic field of the undisturbed medium outside the shell.

6. CONCLUSIONS

As we showed earlier (Borka Jovanović (2012) and references therein), the method for defining a loop border and for determining the values of brightness temperature and surface brightness, which we developed for main Galactic Loops I-VI, could be applicable to all SNRs. Here we use this method in order to:

- determine brightness temperature borders of the Lupus Loop at 1420 and 408 MHz,
- calculate the mean radio spectral index between the specified frequencies, as well as the distribution of indices across the face of this remnant,
- study the correlation between the radio spectral index distribution and the corresponding polarized intensity distribution within the given borders.

In the frequency range under consideration synchrotron radiation dominates the spectrum. We used the radio spectral index to study the radiation mechanism of this radio source. The value obtained for the spectral index (which is > 0.1) confirmed non-thermal emission of radiation for this source. The main disagreement in the measured values can probably be caused by differences in the chosen area for Lupus Loop border. These new observations yielded value of α greater than Milne & Dickel (1974). Besides the nature of the radiation, we also showed how spectral index varies across the face of the remnant.

Taking into account that SNRs radiate non-thermal (synchrotron) radiation which is mainly caused by the magnetic field, which on the other hand is also responsible for the polarization of radiation, we supposed that there exists the connection between the polarization and radio spectral index α, which we then showed.

We can conclude that spectral index significantly varies across the Lupus Loop. Over the time, the synchrotron spectral index becomes steeper (gets greater value, i.e. loops steepen as they age). The boundary of the Lupus Loop is not well defined and the ISM is rather inhomogeneous. That is why there are significant variations in spectral indices α over the loop area.

Acknowledgments. This research is part of the project 176003 "Gravitation and the large scale structure of the Universe" supported by the Ministry

of Education, Science and Technological Development of the Republic of Serbia.

REFERENCES

Borka, V. 2006, Book of contributed papers of the 23^{rd} SPIG, p. 599
Borka, V., Milogradov-Turin, J., & Urošević, D. 2006, Publ. Astron. Obs. Belgrade, 80, 61
Borka, V., 2007, MNRAS, 376, 634
Borka, V., Milogradov-Turin, J., & Urošević, D. 2008, Astron. Nachr., 329, 397
Borka Jovanović, V., & Urošević, D. 2008, Publ. Astron. Obs. Belgrade, 84, 459
Borka Jovanović, V., & Urošević, D. 2009a, Astron. Nachr., 330, 741
Borka Jovanović, V., & Urošević, D. 2009b, Publ. Astron. Obs. Belgrade, 86, 101
Borka Jovanović, V., & Urošević, D. 2010, Journ. Phys: Conf. Ser., 257, 012030
Borka Jovanović, V., & Urošević, D. 2011, Rev. Mex. AA, 47, 159
Borka, D., Borka Jovanović, V., & Urošević, D. 2012, Rev. Mex. AA, 48, 53
Borka Jovanović, V. 2012, Publ. Astron. Obs. Belgrade, 91, 121
Borka Jovanović, V., Borka, D., Skeoch, R., & Jovanović, P. 2012, Publ. Astron. Obs. Belgrade, 91, 255
Colomb, F. R., & Dubner, G. 1982, A&A, 112, 141
Davies, R. D., Dickinson, C., Banday, A. J., Jaffe, T. R., Gorski, K. M., & Davis, R. J. 2006, MNRAS, 370, 1125
Dwarakanath, K. S., & Udaya Shankar, N. 1990, J. Astrophys. Astr. 11, 323
Green, D. A. 2014a, Bull. Astr. Soc. India, 42, 47
Green, D. A. 2014b, A Catalogue of Galactic Supernova Remnants (2014 May version), Astrophysics Group, Cavendish Laboratory, Cambridge, United Kingdom (available at `http://www.mrao.cam.ac.uk/surveys/snrs/`)
Guzman, A. E., May, J., Alvarez, H., & Maeda, K. 2011, A&A, 525, A138
Haslam, C. G. T, Salter, C. J, Stoffel, H, & Wilson, W. E. 1982, A&AS, 47, 1
Heiles, C. 1998, in Lecture Notes in Physics: The Local Bubble and Beyond, 506, Proc. of IAU 166, eds. Breitschwerdt, D., Freyberg, M. J., & Truemper, J., p. 229
Kaplan, D. L., Gaensler, B. M., Kulkarni, S. R., & Slane, P. O. 2006, ApJS, 163, 344
Leahy, D. A., Nousek, J., & Hamilton, A. J. S. 1991, Astrophys., J., 374, 218
Milne, D. K. 1971, Aust. J. Phys., 24, 757
Milne, D. K., & Dickel, J. R. 1974, Aust. J. Phys., 27, 549
Ozaki, M., Koyama, K., Ueno, S., & Yamauchi, S. 1994, Publ. Astron. Soc. Japan, 46, 367
Platania, P., Burigana, C., Maino, D., Caserini, E., Bersanelli, M., Cappellini, B., & Mennella, A. 2003, A&A410, 847
Reich, P., Testori, J. C., & Reich, W. 2001, A&A, 376, 861
Shinn, J.-H., Min, K. W., Lee, C.-N., Edelstein, J., Korpela, E. J., Welsh, B. Y., Han, W., Nam, U.-W., Jin, H., & Lee, D.-H. 2006, ApJ, 644, L189
Spoelstra, T. A. Th. 1973, A&A, 24, 149
Testori, J. C., Reich, P., & Reich, W. 2008, A&A, 484, 733
Toor, A. 1980, A&A, 85, 184
Urošević, D., & Borka Jovanović, V. 2011, Open Astronomy Journal, 4, 218
Vidal, M., Dickinson, C., Davies, R. D., & Leahy, J. P. 2015, MNRAS, 452, 656

Vidal, M. 2016, Diffuse radio foregrounds: All-sky polarisation and anomalous microwave emission, Springer Theses, Springer International Publishing, Switzerland

Zhang, X., Zheng, Y., Landecker, T. L., & Higgs, L. A. 1997, A&A, 324, 641

Vesna Borka Jovanović and Duško Borka: Atomic Physics Laboratory (040), Vinča Institute of Nuclear Sciences, University of Belgrade, P.O. Box 522, 11001 Belgrade, Serbia.

Predrag Jovanović: Astronomical Observatory, Volgina 7, P.O. Box 74, 11060 Belgrade, Serbia.